Structural and optical properties of $Al_{1-x}In_xN$ epilayers on GaN template grown by metalorganic chemical vapor deposition*

Lu Guo-Jun(卢国军)[a], Zhu Jian-Jun(朱建军)[a]†, Jiang De-Sheng(江德生)[a], Wang Yu-Tian(王玉田)[a], Zhao De-Gang(赵德刚)[a], Liu Zong-Shun(刘宗顺)[a], Zhang Shu-Ming(张书明)[a], and Yang Hui(杨 辉)[a][b]

[a] *State Key Laboratory on Integrated Optoelectronics, Institute of Semiconductors, the Chinese Academy of Sciences, P.O. Box 912, Beijing* 100083, *China*

[b] *Suzhou Institute of Nano-tech and Nano-bionics, the Chinese Academy of Sciences, Suzhou* 215123, *China*

(Received 24 March 2009; revised manuscript received 2 June 2009)

This paper reports that $Al_{1-x}In_xN$ epilayers were grown on GaN template by metalorganic chemical vapor deposition with an In content of 7%–20%. X-ray diffraction results indicate that all these $Al_{1-x}In_xN$ epilayers have a relatively low density of threading dislocations. Rutherford backscattering/channeling measurements provide the exact compositional information and show that a gradual variation in composition of the $Al_{1-x}In_xN$ epilayer happens along the growth direction. The experimental results of optical reflection clearly show the bandgap energies of $Al_{1-x}In_xN$ epilayers. A bowing parameter of 6.5 eV is obtained from the compositional dependence of the energy gap. The cathodoluminescence peak energy of the $Al_{1-x}In_xN$ epilayer is much lower than its bandgap, indicating a relatively large Stokes shift in the $Al_{1-x}In_xN$ sample.

Keywords: metalorganic chemical vapor deposition, $Al_{1-x}In_xN$, gradual variation in composition, optical reflectance spectra

PACC: 6855, 0785, 4180G, 7865K

1. Introduction

The III-nitride semiconductors such as GaN, AlN, InN and their alloys have received much attention because of their wide range of bandgap energy, high thermal conductivity, large piezoelectricity and high thermal and chemical stability. Among the III–nitride alloys, $Al_{1-x}In_xN$ is a potential candidate for GaN-based devices. One of the major advantages is that $Al_{1-x}In_xN$ has the largest tunability in the bandgap as the bandgap is 6.2 eV for AlN and 0.7 eV for InN. The spectral range can cover deep ultraviolet to infrared if AlInN is taken as the active layer of light emitters, detectors or laser diodes. At the same time, $Al_{1-x}In_xN$ also has the largest miscibility in the lattice parameter, which enables it to be lattice matched to GaN when In content is close to 17.1%[1] and to other III–nitride alloys by adjusting its composition. Thus a strain-free heterostructure with low dislocation density can be obtained. $Al_{1-x}In_xN$/GaN heterostructure has been applied to highly reflective Bragg mirrors[2,3] and high electron mobility transistor devices.[4,5] However, in contrast, little attention has been paid to the structural and optical properties of $Al_{1-x}In_xN$ ternary alloy in comparison with InGaN and AlGaN alloys despite its potential applications, since the growth of $Al_{1-x}In_xN$ is extremely difficult due to the large difference of covalence bond length and growth temperature between AlN and InN.[6,7] Until now, there has been a large discrepancy in the reported properties of $Al_{1-x}In_xN$, especially its optical properties.[8–14] The reasons may be related to the growth and characterization technologies and different crystalline quality.

In this work, we have grown $Al_{1-x}In_xN$ epilayers on GaN template by mtalorganic chemical vapor deposition (MOCVD) with In content of 7%–20%. The crystalline quality, the In content and the compositional variation along the growth direction of $Al_{1-x}In_xN$ epilayers were investigated by x-ray diffraction (XRD) and Rutherford backscattering/channeling (RBS/C) measurements. The band-

*Project supported by the National Natural Science Foundation of China (Grant Nos. 60776047, 60506001, 60476021, 60576003 and 60836003).

†Corresponding author. E-mail: jjzhu@red.semi.ac.cn

© 2010 Chinese Physical Society and IOP Publishing Ltd

gap and optical emission properties of $Al_{1-x}In_xN$ epilayers were also characterized by optical reflectance spectra and cathodoluminescence (CL), respectively. Based on these results, the bowing parameter of the bandgap of $Al_{1-x}In_xN$ epilayers was estimated. A large value of Stokes shift was observed in the $Al_{1-x}In_xN$ samples.

2. Experimental procedure

The materials were grown by low pressure MOCVD using Thomas Swan Scientific Equipment 3×2 CCS-MOCVD. First, a 2-μm thick GaN template layer was grown on a 25-nm-thick low-temperature GaN buffer on the (0001) sapphire substrate, where trimethylgallium (TMGa) and ammonia (NH_3) were used as the source materials and hydrogen (H_2) as the carrier gas. Then about 150-nm-thick $Al_{1-x}In_xN$ epilayer was grown on GaN template. The thickness was estimated by the *in situ* laser reflection monitor. NH_3, trimethylaluminum (TMAl) and trimethylindium (TMIn) were used as precursors for N, Al and In, respectively. The carrier gas was changed from H_2 to nitrogen (N_2). In order to obtain a relatively high In content in $Al_{1-x}In_xN$ epilayers, TMIn to TMAl molar flow rate ratio was chosen to be high and excessive, i.e. the flow rates of TMIn and TMAl were 20 μmol/min and 5 μmol/min, respectively. The five investigated $Al_{1-x}In_xN$ samples were grown at temperature between 740 °C and 820 °C and pressure between 60 Torr and 120 Torr (1 Torr = 133 Pa).

Triple-axis XRD measurements were performed on a Rigaku SLX-1A diffracter equipped with a Si (220) analyzer to evaluate crystalline quality of $Al_{1-x}In_xN$ epilayers. A collimated 1.57 MeV He^+ beam was used for RBS/C measurements to determine the composition of $Al_{1-x}In_xN$ epilayers. During RBS/C measurements, the samples were mounted on a high-precision (0.01°) three-axis goniometer in vacuum chamber so that the orientation of measured samples relative to the He^+ beam could be precisely controlled. The backscattered particles were detected by an Au–Si barrier detector. The detection angle was 167.8° and the energy resolution was around 14 keV. Optical reflectance measurements were carried out with an incident angle 6° on a Perkin Elmer LAMBDA 950 UV-VIS spectrophotometer. Low-temperature CL measurements were performed at 5 K with an Oxford Mono-CL2 and He-cooling stage. A grating monochromator and a cooled charge-coupled device array were used to disperse and detect the CL signal, respectively.

3. Results and discussion

To evaluate the crystalline quality of $Al_{1-x}In_xN$ epilayers, the triple-axis XRD measurements, including both ω–2θ scan and ω scan [x-ray rocking curves (XRC)], were carried out. Figure 1(a) shows the triple-axis (0002) ω–2θ XRD patterns of $Al_{1-x}In_xN$ epilayers with different In content x, whose composition is determined by RBS as will be described in detail later. In Fig. 1 the peaks at 34.56° originate from GaN templates and all $Al_{1-x}In_xN$ peaks locate at the right side of GaN peaks. The peak of $Al_{1-x}In_xN$ epilayers shifts to low angle with increasing In content. No peak splitting is observed, indicating that $Al_{1-x}In_xN$ epilayers are not affected macroscopically by phase separation. Furthermore, it is seen that the full width at half maximum (FWHM) of the peak of $Al_{1-x}In_xN$ epilayers becomes broader with increasing In content, from 314 arcsec with In content of 7.4 % to 720 arcsec with In content of 20.1 %. Since all measured $Al_{1-x}In_xN$ epilayers have almost the same thickness, the difference in the broadening of the ω–2θ diffraction peaks of $Al_{1-x}In_xN$ should mainly arise from the inhomogeneous strain. In fact, the compositional inhomogeneity of the film should be the major factor contributing to the inhomogeous strain in the alloy layer.[15] Accordingly, the above-mentioned result suggests that the compositional fluctuation of $Al_{1-x}In_xN$ epilayers becomes stronger when In content increases. Figure 1(b) shows the FWHMs of XRCs for (0002) and (10–12) $Al_{1-x}In_xN$ epilayers with different In content x. The FWHM of XRCs for (10–12) $Al_{1-x}In_xN$ epilayer with In content of 20.1% cannot be determined since two peaks of GaN and $Al_{1-x}In_xN$ skew (10–12) diffraction are overlapped. It is known that the symmetric (0002) reflection is most sensitive to the density of threading dislocations (TDs) with a screw component (screw and mixed TDs), while the skew (10–12) diffraction is affected by the density of all types of TDs (screw, edge and mixed TDs).[16] The FWHM of XRCs for (0002) of all five samples is about 350 arcsec, and the FWHM of XRCs for (10–12) of these samples is about 600 arcsec except for the $Al_{1-x}In_xN$ epilayer with In content of 7.4%. This result shows that these $Al_{1-x}In_xN$ epilayers have a relatively low density of TDs.

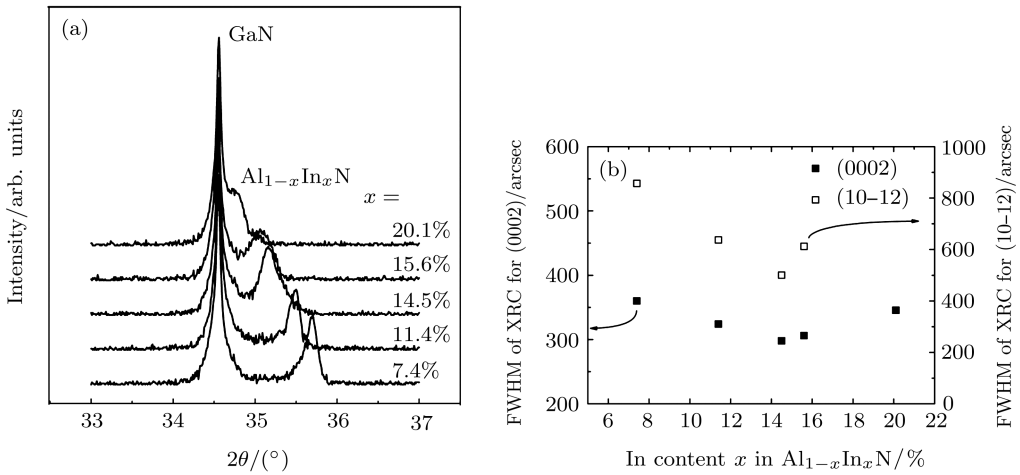


Fig. 1. (a) Triple-axis (0002) ω–2θ XRD patterns. (b) FWHMs of XRCs for (0002) and (10–12) of $Al_{1-x}In_xN$ epilayers with different In content x.

The composition of $Al_{1-x}In_xN$ epilayers can be directly determined by using RBS/C measurements. The RBS measurements can determine In content without the influence of strain and thus are more reliable.[17] Figures 2(a)–2(c) show the random RBS spectra and fitted curves for three representative $Al_{1-x}In_xN$ epilayers. The arrows labeled as "In" and "Al" indicate the energies for backscattering from In and Al atoms at the $Al_{1-x}In_xN$ surface. The simulation results of random RBS spectra given by the RUMP program[18] (as shown by solid curves in Figs. 2(a)–2(c)) indicate that the average In contents $x_{\rm RBS}$ in the $Al_{1-x}In_xN$ epilayers are 11.4%, 14.5% and 20.1%, respectively. Based on the data of (0002) XRD ω–2θ scans, the In content $x_{\rm XRD}$ can also be calculated by using the angular separation of GaN and $Al_{1-x}In_xN$ peaks according to Vegard's law when we assume that the $Al_{1-x}In_xN$ epilayers are fully relaxed.[19,20] It is found that the In contents determined by XRD do not agree very well with the values obtained by RBS measurements. The deviation of the XRD data from the RBS ones suggests that the $Al_{1-x}In_xN$ epilayers are not fully relaxed. Therefore, the measured $Al_{1-x}In_xN$ layers are actually either fully strained or partially relaxed. It is found that the composition data obtained by RBS and XRD for the layers with In content close to 17% do not differ each other too much. This is reasonable because such layers have a lattice constant close to the lattice-matched $Al_{1-x}In_xN$ with In content of 17.1%,[1] and a smaller strain has a less influence on the result of XRD measurements. It is found that the In content $x_{\rm XRD}$ is underestimated for the $Al_{1-x}In_xN$ epilayers with In content $x < 17\%$ due to the tensile strain, while overestimated for the epilayers with In content $x > 17\%$ due to the compressive strain as shown in Fig.2(d).

Though the phase separation is not observed macroscopically from the triple-axis (0002) ω–2θ XRD patterns in Fig. 1(a), it is found that the compositions of Al and In vary a little in the growth direction of the $Al_{1-x}In_xN$ epilayer from an analysis of RBS spectra. The In content is higher during the initial stages of $Al_{1-x}In_xN$ growth on GaN template, and decreases with increasing film thickness. It has been reported[21,22] that biaxial strain in InGaN or AlGaN films grown on GaN layer may result in a pulling effect on the In or Al compositions. It is believed that In or Al atoms will be expelled from the epilayer during the initial stage of the growth to reduce the strain energy from the thermodynamic aspect. In the case of the $Al_{1-x}In_xN$ epilayers with $x \leq 17\%$[1] grown on GaN template, the in-plane lattice constant of $Al_{1-x}In_xN$ epilayer is smaller than that of GaN template. The Al atoms will be pulled out of the film due to the tensile biaxial strain in the initial stage of $Al_{1-x}In_xN$ growth. It results in a deposition of the epilayer with a lower Al and a higher In content. Then a gradual strain reduction in the grown $Al_{1-x}In_xN$ epilayer will take place as the growth continues, and the subsequently deposited $Al_{1-x}In_xN$ epilayer will have a lower In content. It is what has been observed for the samples of $Al_{0.89}In_{0.11}N$ and $Al_{0.85}In_{0.15}N$. For the $Al_{1-x}In_xN$ epilayers with $x \geq 17\%$,[1] the In content distribution along the growth direction should be opposite to the case of $Al_{1-x}In_xN$ epilayer with $x \leq 17\%$. However, for the sample $Al_{0.80}In_{0.20}N$, the In content is also found to be higher at the initial stage of $Al_{1-x}In_xN$ growth. This result is not expected from the compositional pulling effect. Lorenz *et al.* have observed a similar abnormality

in $Al_{1-x}In_xN$ growth with $x > 19\%$. This phenomenon is possibly related to the effect that in $Al_{1-x}In_xN$ alloy film the compressive strain may facilitate the In incorporation and thus the relaxed surface layer contains less InN.[23]

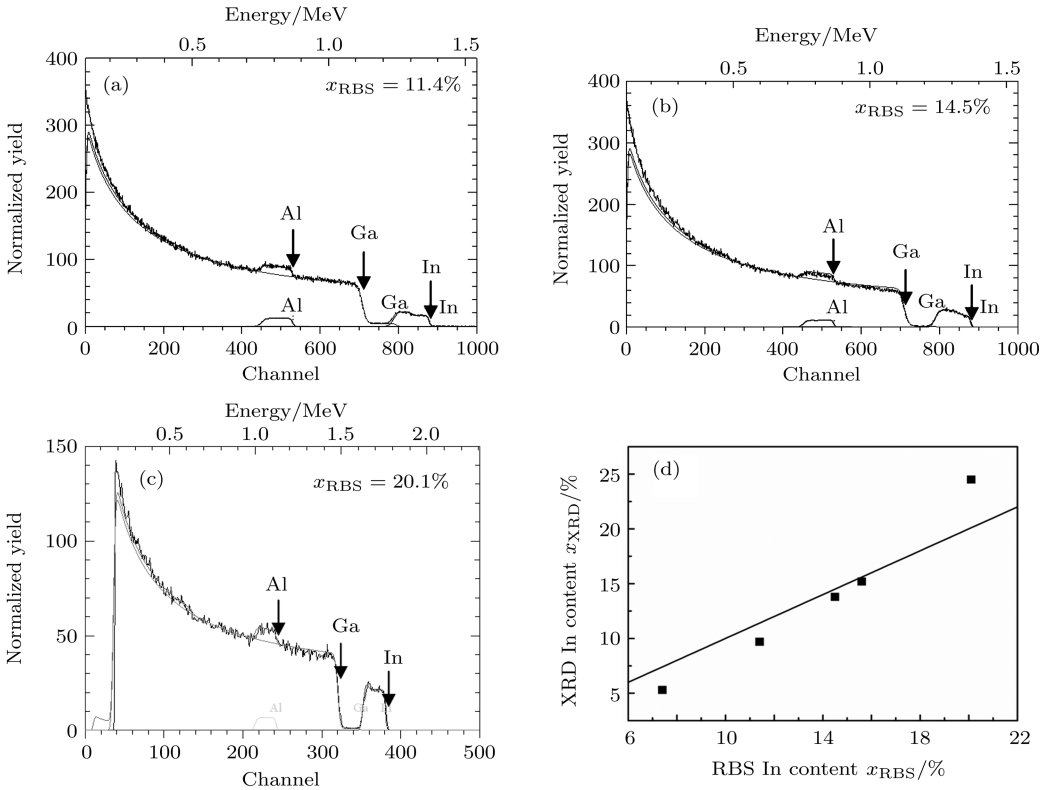


Fig. 2. The RBS spectra of (a) $Al_{0.89}In_{0.11}N$, (b) $Al_{0.85}In_{0.15}N$, (c) $Al_{0.80}In_{0.20}N$ and (d) x_{XRD} as a function of x_{RBS}, where x_{RBS} and x_{XRD} indicate the In content determined by using RBS and XRD experiments, respectively. One-to-one correspondence between RBS and XRD results is represented by the line.

In addition, the reciprocal space mapping (RSM) was used to evaluate the strain state in $Al_{1-x}In_xN$ epilayers. As shown in Fig. 3, the RSM of asymmetric (–1015) reflection of the $Al_{1-x}In_xN$ sample with In content of 7.4% was performed. The reciprocal lattice points (RLPs) for both GaN template and $Al_{1-x}In_xN$ epilayer are visible on the map. The fully relaxed growth and pseudomorphic growth of $Al_{1-x}In_xN$ are described by solid and dotted lines, respectively. The calculated relaxation line is shown by dashed line.[24] The result of RSM reveals that the $Al_{1-x}In_xN$ epilayer is in a partially relaxed state. Furthermore, it is observed that the RLP of $Al_{1-x}In_xN$ has a broadening along both the relaxation line and the line directed towards the GaN template RLP in the RSM, suggesting that the gradients of both strain and composition exist in the epilayer.[25] The results are in accord with ones of the above-mentioned XRD and RBS measurements.

For $Al_{1-x}In_xN$/GaN/sapphire samples with In content in the range of 7%–20%, the usual optical transmission measurement is not suitable for measuring the bandgap of $Al_{1-x}In_xN$ epilayers since the bandgap energy of $Al_{1-x}In_xN$ is larger than that of GaN template. The thick GaN template is not transparent in the spectral range of intrinsic absorption of $Al_{1-x}In_xN$. In order to estimate the optical bandgap of the $Al_{1-x}In_xN$ epilayers, we carried out the optical reflectance measurements at room temperature, as shown in Fig. 4. It is found that the reflection spectrum is composed of two independent multiple interference fringes having shorter and longer periods caused by GaN template and $Al_{1-x}In_xN$ epilayer, respectively. It is noted that when the photon energy exceeds the bandgap of the material, the amplitude of the interference fringes will quickly disappear due to a strong intrinsic absorption above the bandgap. Therefore, the bandgap of GaN template

can be estimated from the high-energy edge of the shorter period interference fringes, while the bandgap of $Al_{1-x}In_xN$ epilayer can be estimated from the high-energy edge of the longer period interference fringes.[10] In Fig. 4, the dashed line and the downward arrows show the energy position of the bandgap of GaN template and $Al_{1-x}In_xN$ epilayers, respectively. The optical bandgaps are thus estimated to be 4.04 eV, 4.17 eV, 4.21 eV, 4.43 eV and 5.24 eV for the samples of $Al_{0.80}In_{0.20}N$, $Al_{0.84}In_{0.16}N$, $Al_{0.85}In_{0.15}N$, $Al_{0.89}In_{0.11}N$ and $Al_{0.93}In_{0.07}N$ epilayers, respectively.

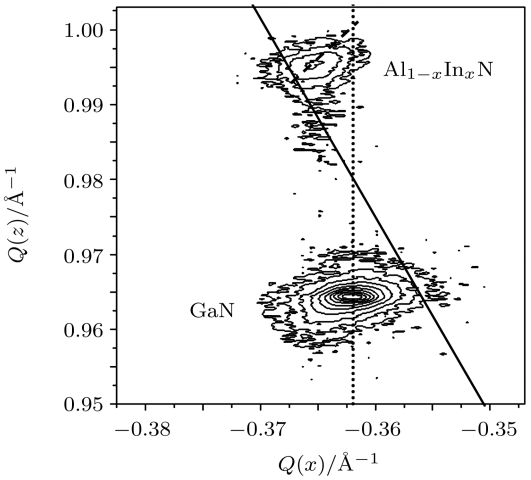


Fig. 3. The RSM of asymmetric (–1015) reflection for the $Al_{1-x}In_xN$ sample with In content of 7.4%. The fully relaxed growth and the pseudomorphic growth of $Al_{1-x}In_xN$ are described by solid and dotted lines, respectively. The calculated relaxation line is shown by dashed line.

Figure 5 shows a dependence of the bandgap energy of $Al_{1-x}In_xN$ epilayers on the In content x, where some reported representative results of the bandgap for $Al_{1-x}In_xN$ epilayers by MOCVD are shown. The filled circles, the open squares and the filled triangles are the results of Onuma *et al.*,[10] Carlin *et al.*[3] and Yamaguchi *et al.*,[11] respectively. Our experimental data are shown by filled stars. We can see that there is a large discrepancy between the results of Yamaguchi *et al.* and other results due to the high concentration of electron in their samples which modified the bandgap of $Al_{1-x}In_xN$.[11] The bandgap energy ($E_g(x)$) of $Al_{1-x}In_xN$ can be expressed as $E_g(x) = xE_{g,InN} + (1-x)E_{g,AlN} - bx(1-x)$, where $E_{g,InN} = 0.7$ eV and $E_{g,AlN} = 6.2$ eV are the bandgap energies of AlN and InN respectively, and b represents the bowing parameter. Based on our data the bowing parameter b is estimated by simulation to be 6.5 eV, which is larger than those previously reported bowing parameter of 3.1 eV[10] or 6 eV.[3,12] The difference among the experimental values for the bowing parameter of $Al_{1-x}In_xN$ films may be due to the internal and/or external microstructure, such as stress, defect density and fluctuations in the local In content of $Al_{1-x}In_xN$.

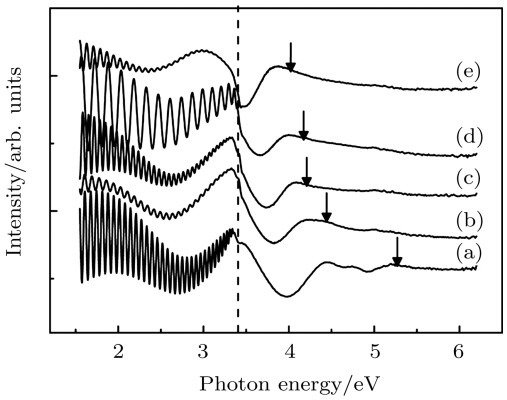


Fig. 4. Room-temperature reflectance spectra of $Al_{1-x}In_xN$ /GaN/sapphire samples with different In content x of (a) 7.4%, (b) 11.4%, (c) 14.5%, (d) 15.6% and (e) 20.1%. The downward arrows show the energy position of E_g of $Al_{1-x}In_xN$.

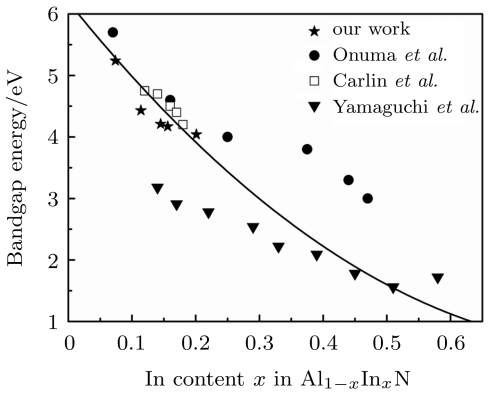


Fig. 5. Dependence of the bandgap energy of $Al_{1-x}In_xN$ on In content x. Our experimental data are shown by filled stars. The filled circles, the open squares and the filled triangles are the results of Onuma *et al.*, Carlin *et al.* and Yamaguchi *et al.*, respectively. The solid line indicates the fitted curve obtained by using the bowing parameter $b = 6.5$ eV.

Low-temperature CL measurements have also been carried out on the $Al_{1-x}In_xN$ sample with In content of 14.5%, as shown in Fig. 6. The sample shows four main CL peaks. The peaks at 3.50 eV, 3.28 eV and 3.19 eV are related to the underlying GaN template. The peak at 3.82 eV is related to the $Al_{1-x}In_xN$ epilayer, which exhibits an FWHM of ∼385 meV. It is important to note that the peak energy of AlInN emission observed in CL does not correspond to the actual bandgap of the $Al_{0.85}In_{0.15}N$ epilayer determined by optical reflectivity measurements as shown in Fig. 6

as a comparison. From the CL and reflectance spectra, an energy difference of about 390 meV is deduced, corresponding to a relatively large Stokes shift. The energy difference may be even larger if CL is measured at room temperature. A large Stokes shift between the absorption edge and the interband luminescence peak is often observed for the alloy film samples. Its value is related to the compositional fluctuation and spatial inhomogeneity of the alloy film. A large Stokes shift was reported commonly in previous literatures for $Al_{1-x}In_xN$ films.[10,12] For example, the Stokes shift was reported to be about 500 meV for some high quality samples.[3] For $Al_{1-x}In_xN$ samples,

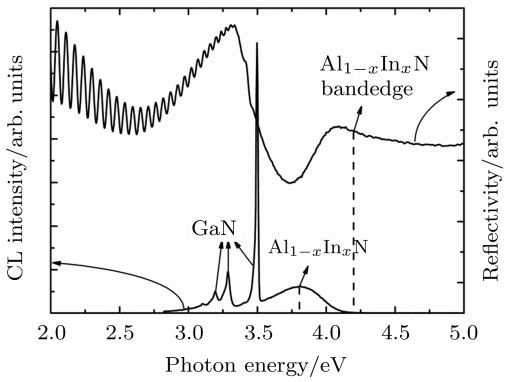


Fig. 6. Low-temperature CL and room-temperature reflectance spectrum of $Al_{1-x}In_xN$/GaN/sapphire sample with In content of 14.5%.

the Stokes shift is normally larger in comparison with that usually measured in AlGaN or low indium content InGaN alloys,[26−28] suggesting that the strong composition fluctuation in $Al_{1-x}In_xN$ caused by the large difference in chemical bonds between InN and AlN.

4. Conclusion

$Al_{1-x}In_xN$ epilayers were grown on GaN template by MOVCD with the In content of 7%–20%. The epilayers were characterized by XRD, RBS and optical reflectance spectra as well as CL. The XRD results indicate that all these $Al_{1-x}In_xN$ epilayers have a relatively low density of TDs. The RBS/C measurements show that a gradual variation in the compositions of the $Al_{1-x}In_xN$ epilayer happens along the growth direction. The experimental results of optical reflection can clearly show the bandgap energy of $Al_{1-x}In_xN$ epilayers. A bowing parameter of 6.5 eV is obtained from the compositional dependence of the energy gap. The obtained CL peak energy of the $Al_{1-x}In_xN$ epilayer is much lower than the bandgap, indicating a relatively large Stokes shift in the $Al_{1-x}In_xN$ sample.

Acknowledgements

The authors would like to thank Beijing Synchrotron Radiation Facility for the assistance in thin film characterization, Dr. G. Husnain (School of Physics, Peking University) for the RBS measurements and Uwe Jahn (Paul-Drude-Institute for Solid State Electronics Berlin) for the CL measurements.

References

[1] Lorenz K, Franco N, Alves E, Watson I M, Martin R W and O'Donnell K P 2006 *Phys. Rev. Lett.* **97** 085501

[2] Carlin J F and Ilegems M 2003 *Appl. Phys. Lett.* **83** 668

[3] Carlin J F, Zellweger C, Dorsaz J, Nicolay S, Christmann G, Feltin E, ButtéR and Grandjean N 2005 *Phys. Stat. Sol.* B **242** 2326

[4] Dadgar A, Schulze F, Blasing J, Diez A, Krost A, Neuburge M, Kohn E, Daumiller I and Kunze M 2004 *Appl. Phys. Lett.* **85** 5400

[5] Gonschorek M, Carlin J F, Feltin E, Py M A and Grandjean N 2006 *Appl. Phys. Lett.* **89** 062106

[6] Matsuoka T 1997 *Appl. Phys. Lett.* **71** 105

[7] Koukitu A and Seki H 1996 *Jpn. J. Appl. Phys.* **35** L1638

[8] Kim K S, Saxler A, Kung P, Razeghi M and Lim K Y 1997 *Appl. Phys. Lett.* **71** 800

[9] Lukitsch M J, Danylyuk Y V, Naik V M, Huang C, Auner G W, Rimai L and Naik R 2001 *Appl. Phys. Lett.* **79** 632

[10] Onuma T, Chichibu S F, Uchinuma Y, Sota T, Yamaguchi S, Kamiyama S, Amano H and Akasaki 2003 *J. Appl. Phys.* **94** 2449

[11] Yamaguchi S, Kariya M, Nitta S, Kato H, Takeuchi T, Wetzel C, Amano H and Akasaki I 2000 *Appl. Phys. Lett.* **76** 876

[12] Wang K, Martin R W, Amabile D, Edwards P R, Hernandez S, Nogales E, O'Donnell K P, Lorenz K, Alves E, Matias V, Vantomme A, Wolverson D and Watson I M 2008 *J. Appl. Phys.* **103** 073510

[13] Oh T S, Kim J O, Jeong H, Lee Y S, Nagarajan S, Lim K Y, Hong C H and Suh E K 2008 *J. Phys.* D: *Appl. Phys.* **41** 095402

[14] Iliopoulos E, Adikimenakis A, Giesen C, Heuken M and Georgakilas A 2008 *Appl. Phys. Lett.* **92** 191907

[15] O'Donnell K P, Martin R W and Middleton P G 1999 *Phys. Rev. Lett.* **82** 237

[16] Heying B, Wu X H, Keller S, Li Y, Kapolnek D, Keller B P, DenBarrs S P and Speck J S 1996 *Appl. Phys. Lett.* **68** 643

[17] Wu M F, Vantomme A, Hogg S, Langouche G, Vander Strich W, Jacobs K and Moerman I 2001 *Nucl. Instrum. Methods Phys. Res.* B **174** 181

[18] Doolittle L R 1985 *Nucl. Instrum. Methods Phys. Res.* B **9** 344

[19] Singh R, Doppalapudi D, Moustakas T D and Romano L T 1997 *Appl. Phys. Lett.* **70** 1089

[20] El-Masty N A, Piner E L, Liu S X and Bedair S M 1998 *Appl. Phys. Lett.* **72** 40

[21] Pereira S, Correia M R, Pereira E, O'Donnell K P, Trager-Cowan C, Sweeney F and Alves E 2001 *Phys. Rev.* B **64** 205311

[22] Lin H Y, Chena Y F, Linb T Y, Shihc C F, Liub K S and Chen N C 2006 *J. Cryst. Growth* **290** 225

[23] Lorenz K, Franco N, Alves E, Pereira S, Watson I M, Martin R W and O'Donnel K P 2008 *J. Cryst. Growth* **310** 4058

[24] Heinke H, Möller M O, Hommel D and Landwehr G 1994 *J. Cryst. Growth* **135** 41

[25] Heinke H, Einfeldt S, Kuhn-Heinrich B, Plahl G, Möller M O and Landwehr G 1995 *J. Phys.* D **28** A104

[26] Cho Y H, Gainer G H, Lam J B, Song J J, Yang W and Jhe W 2000 *Phys. Rev.* B **61** 7203

[27] Sasaki C, Naito H, Iwata M, Kudo H, Yamada Y, Taguchi T, Jyouichi T, Okagawa H, Tadatomo K and Tanaka H 2003 *J. Appl. Phys.* **93** 1642

[28] Chen X X, Teng L H, Liu X D, Huang Q W, Wen J H, Lin W Z and Lai T S 2008 *Acta Phys. Sin.* **57** 3853 (in Chinese)